Electronic Supplementary Material (ESI) for Dalton Transactions.

The controlling role of atmosphere in dawsonite versus gibbsite precipitation from tetrahedral aluminate species

Mateusz Dembowski[†], John S. Loring[†], Mark Bowden[†], Jacob G. Reynolds[‡], Trent R. Graham[†], Kevin M. Rosso[†], and Carolyn I. Pearce[†, #]

[†]Pacific Northwest National Laboratory, Richland, Washington 99352, USA

[‡]Washington River Protection Solutions, LLC, Richland, Washington 93352, USA

[#] Washington State University, Pullman, WA, 99164

Table of Contents

In-situ ATR spectroscopy

20% relative humidity, 400 ppm CO_2

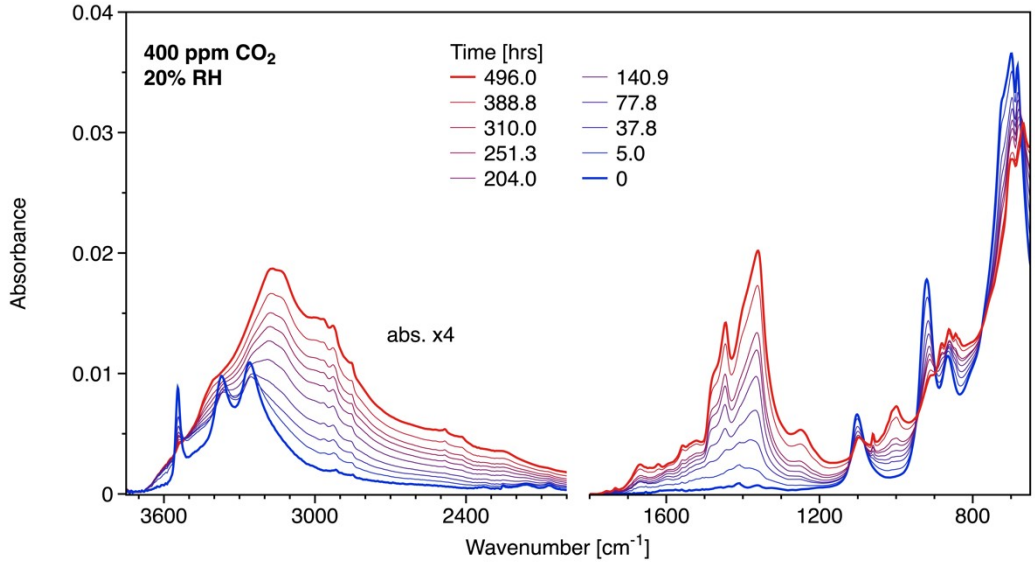

Figure S1. Examples of ATR IR spectra from 650 to 3700 cm^{-1} as a function of time during the reaction of $K_2Al_2O(OH)_6$ in a gas mixture of 400 ppm CO_2 in argon at 25°C and 20 % RH. Spectra have been baseline corrected and area normalized, as described in the Methods section. Note the scale change between low (650-1800 cm^{-1}) and high (2000-3750 cm^{-1}) wavenumber region.

30% relative humidity, 400 ppm CO_2

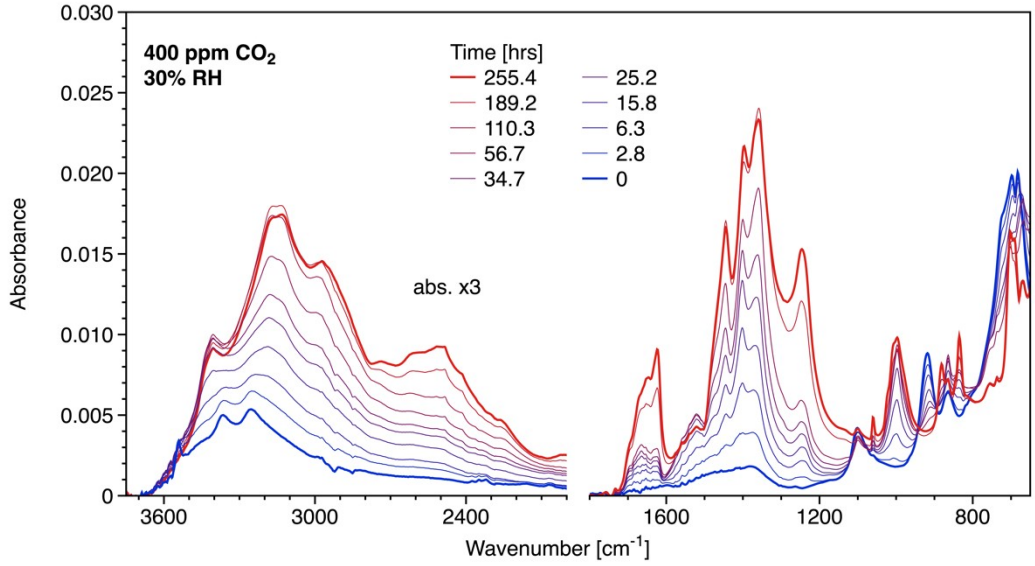

Figure S2. Examples of ATR IR spectra from 650 to 3700 cm^{-1} as a function of time during the reaction of $K_2Al_2O(OH)_6$ in a gas mixture of 400 ppm CO_2 in argon at 25°C and 30 % RH. Spectra have been baseline corrected and area normalized, as described in the Methods section. Note the scale change between low (650-1800 cm^{-1}) and high (2000-3750 cm^{-1}) wavenumber region.

MCR-ALS results

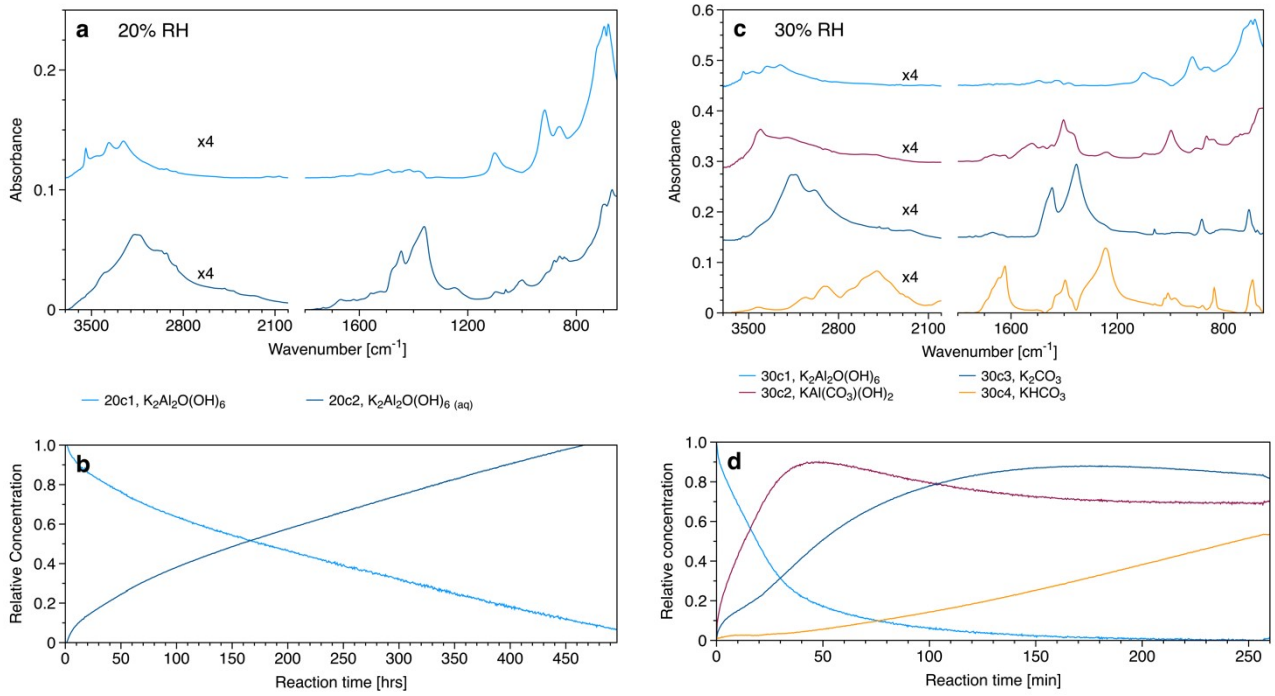

Figure S3. Results of MCR-ALS analyses of ATR IR spectra collected as a function of time during experiments where $K_2Al_2O(OH)_6$ was reacted in a gas mixture of 400 ppm CO_2 in argon at 25°C. Panels (a) and (b) show the spectra and relative concentrations, respectivly, of the components resolved for the experiment carried out at 20% RH. Likewise, panels (c) and (d) are from the experiment at 30% RH. Assignments are given in the legends, and the same color is used in all experiments for components assigned to the same species. The MCR-ALS analyses accounted for better than 99.95% of the variance in the data at each RH

Two unique spectral components were used for the MCR-ALS analysis of the ATR IR data at 20% RH (**Figure S1**), and their spectra are shown in **Figure S3a**. Component 20c1 is the spectrum of the unreacted $K_2Al_2O(OH)_6$ aluminate dimer. The second component 20c2 is assigned to the hydrated form of the aluminate dimer, although significant contributions from the carbonate (CO_3^{2-}) are observed at ca. 1400 cm^{-1}. No other significant components were identified. Attempts to further resolve the second component were unsuccessful. The two components show inverse relative concentration dependence with growth of the hydrated form of the aluminate dimer (with significant carbonate contribution) coinciding with depletion of the starting material. The μXRD analysis confirms retention of $K_2Al_2O(OH)_6$ as the major solid phase present as well as formation of small quantities of K_2CO_3 and $KAl(CO_3)(OH)_2$. Although not resolved by the MCR-ALS analysis, close inspection of the 20c2 spectra reveals a weak shoulder at ca. 3440 cm^{-1} that is consistent with presence of small quantities of $KAl(CO_3)(OH)_2$.

Four spectral components were used for the MCR-ALS analysis of the ATR IR data at 30% RH (**Figure S2**) and their spectra are shown in **Figure S3c**. Component 30c1 is the spectrum of the unreacted $K_2Al_2O(OH)_6$ aluminate dimer. Component 30c2 is assigned to the $KAl(CO_3)(OH)_2$ species, 30c3 to K_2CO_3, and 30c4 to $KHCO_3$. Exposure of $K_2Al_2O(OH)_6$ to 30% RH led to its partial depletion and rapid growth of the K-dawsonite phase accompanied by a slower growth of the carbonate (K_2CO_3) and bicarbonate ($KHCO_3$) phases. It should be noted that interpretation of changes in relative concentrations of different components at 30% (and 20%) should be approached with caution due to slow kinetics and incomplete reaction of the starting material (**Figure S4**) as opposed to reactions at RH>30%. Similarly to results observed at 20% RH, the μXRD results obtained at the end of reaction still indicate $K_2Al_2O(OH)_6$ as the major crystalline phase present. Other identified crystallographic phases include K_2CO_3, $K_2CO_3{\cdot}KHCO_3$, and $KAl(CO_3)(OH)_2$ accounting for all components identified from the IR spectra.

µXRD results

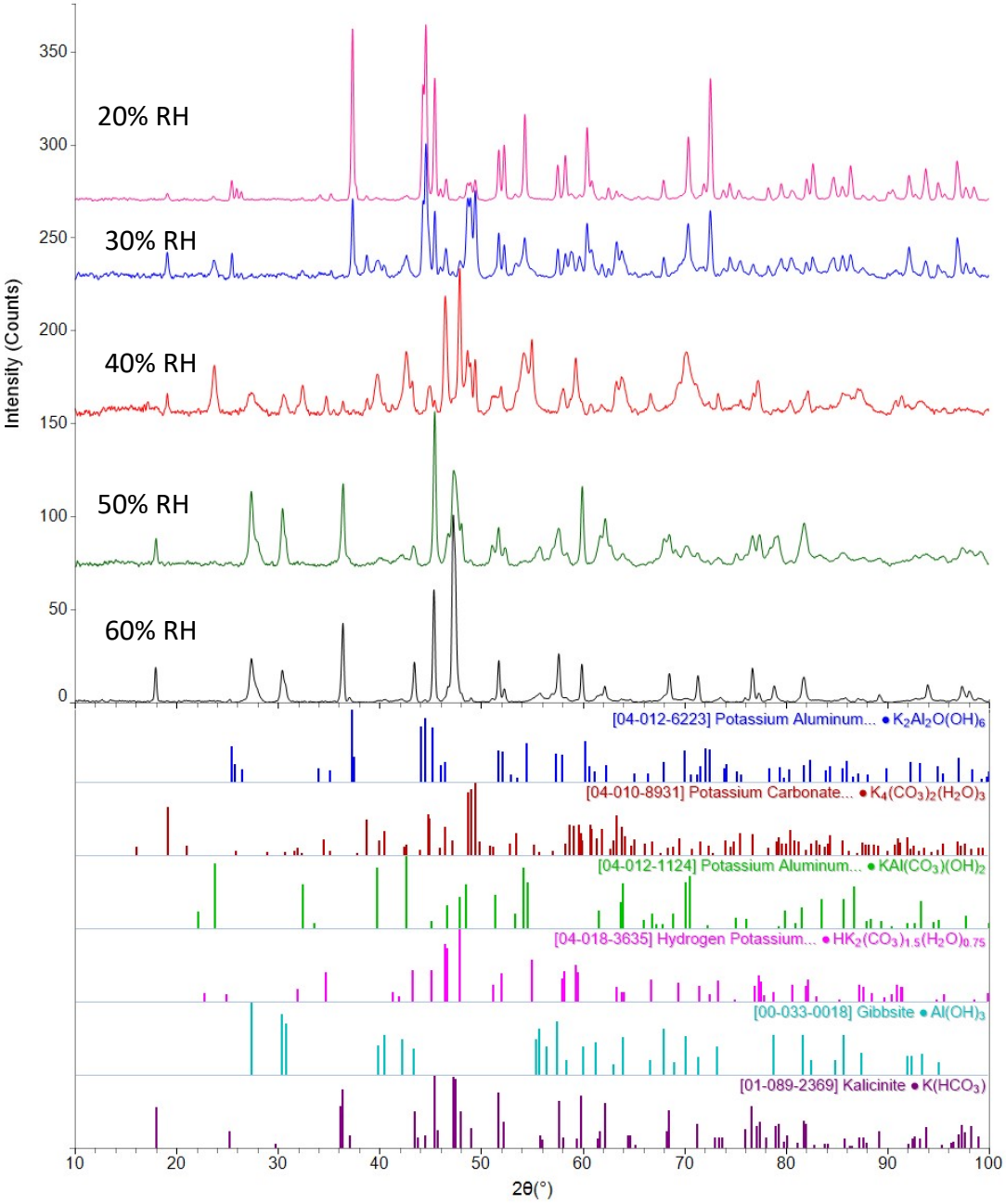

Figure S4. Summary of µXRD analysis of post-reacted samples at RH conditions ranging from 20 (top) to 60% (bottom).

Relative Humidity	crystallographic phases					
	$K_2Al_2O(OH)_6$ 04-012-6223	$KAl(CO_3)(OH)_2$ 04-012-1124	$Al(OH)_3$ 00-033-0018	$KHCO_3$ 01-089-2369	K_2CO_3 04-010-8931	$K_2CO_3{\cdot}KHCO_3$ 04-018-3635
20%	Pr.	Pr.	Abs.	Abs.	Pr.	Abs.
30%	Pr.	Pr.	Abs.	Abs.	Pr.	Pr.

Pr. = present, Abs. = absent

Additional IR analysis

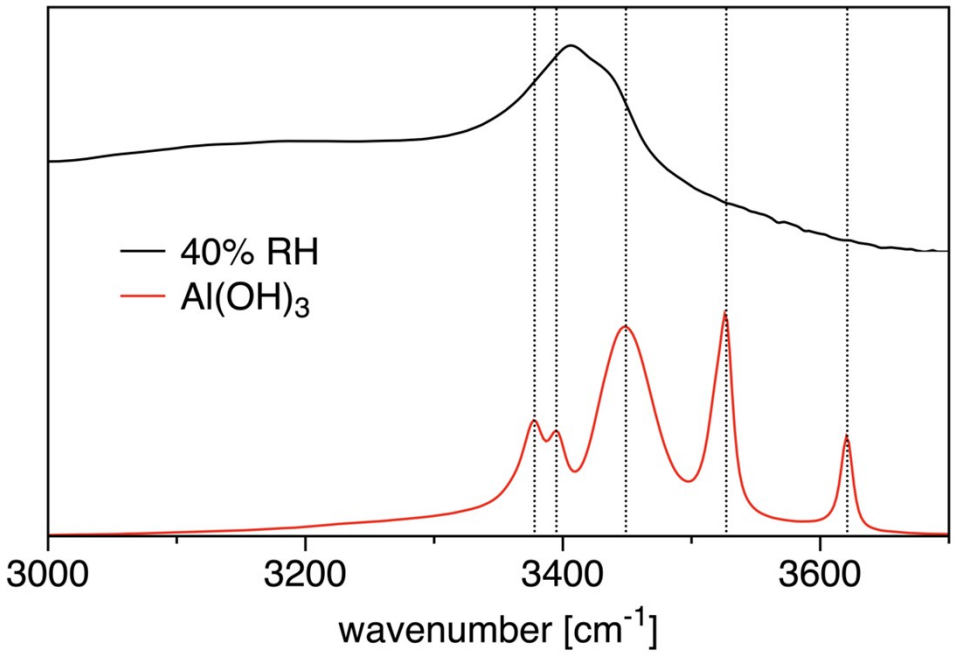

Figure S5. Comparison of IR spectra collected prior to μXRD analysis after reacting at 40% RH (black trace) and that of synthetic $Al(OH)_3$ (red trace) showing characteristic -OH stretching bands. Black dotted lines highlight the positions of bands present in $Al(OH)_3$

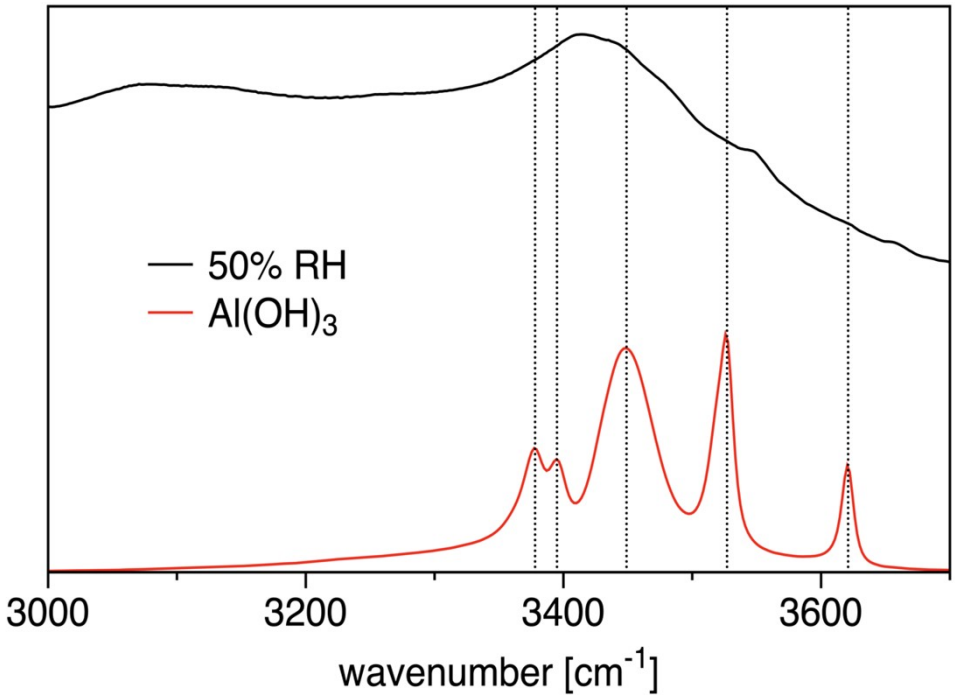

Figure S6. Comparison of IR spectra collected prior to μXRD analysis after reacting at 50% RH (black trace) and that of synthetic $Al(OH)_3$ (red trace) showing characteristic -OH stretching bands. Black dotted lines highlight the positions of bands present in $Al(OH)_3$.

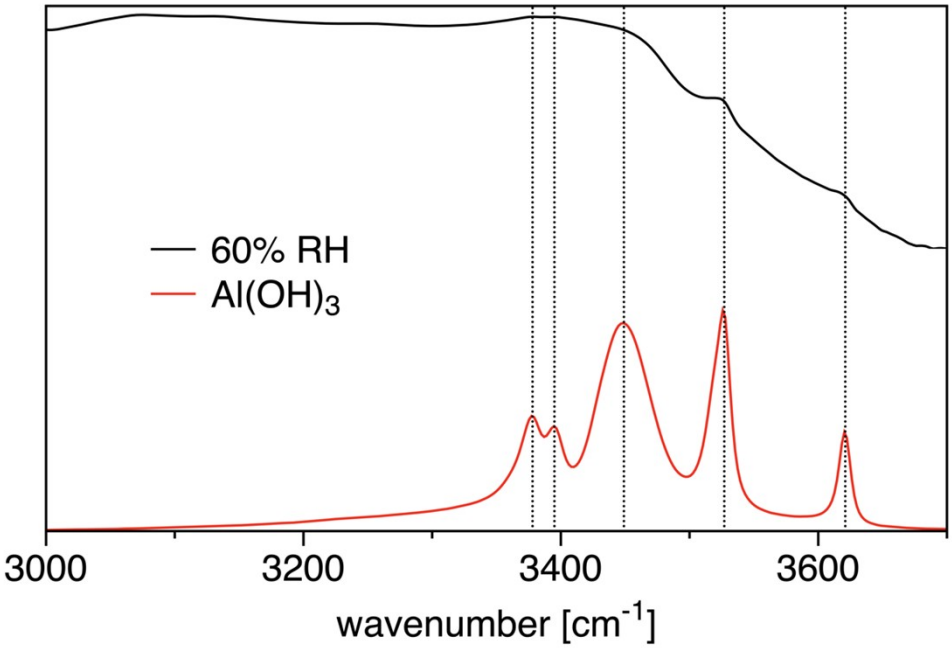

Figure S7. Comparison of IR spectra collected prior to μXRD analysis after reacting at 60% RH (black trace) and that of synthetic $Al(OH)_3$ (red trace) showing characteristic -OH stretching bands. Black dotted lines highlight the positions of bands present in $Al(OH)_3$.